CRITERION DESIGN FOR OPTIMIZING LOW-COST APPROXIMATIONS OF INFINITE-DIMENSIONAL SYSTEMS: TOWARDS EFFICIENT REAL-TIME SIMULATION.

Thomas Hélie [*] **Denis Matignon** [**] **Rémi Mignot** [*]

[*] *Laboratoire des Sciences et Technologie de la Musique et du Son, Equipe Analyse/Synthèse. CNRS UMR 9912 - Ircam, Centre Georges Pompidou. 1, place Igor Stravinsky. 75004 Paris, France.*
Thomas.Helie@ircam.fr, Remi.Mignot@ircam.fr
[**] *Laboratoire Traitement et Communication de l'Information, Département Traitement du Signal et des Images. CNRS UMR 5141 - Télécom Paris. 37-39, rue Dareau 75014 Paris, France.* matignon@tsi.enst.fr

Abstract: Linear systems with irrational transfer functions are difficult to simulate in the time domain. We consider causal systems which can be represented with poles and cuts in some left half-plane of the Laplace domain. Whereas standard interpolation methods yield convergent but high-dimensional approximations, it is possible to derive efficient low-cost approximations thanks to optimization procedures. Defining the criterion (choice of weightening measure, regularization and contraints) is however of utmost importance: this must be carefully designed and driven by each application. Two examples will illustrate the methodology, and a third one will present an extension to a compound system with delays.

Keywords: infinite-dimensional systems, integral representations, non-uniform least-square criterion, constrained and regularized optimization, real-time simulation.

NB: *Results described in § 4.3 are to be submitted to the INPI for a patent.*

1. INTRODUCTION

Real-time simulation of many complex physical systems is an issue that has significantly evolved: as an example, building up a virtual musical instrument has now become within reach on home computers. The purpose of this paper is to shed a new light on some aspects of the methodological process which starts from the equations of the physical model, goes through an exact representation of the solution from which a well-suited approximation is optimized, and, ends up with real-time simulations.

Standard methods of numerical analysis of PDEs are not so well oriented towards real-time simulation: given a prescribed accuracy, the order of the finite-dimensional model, coming e.g. from finite

difference schemes or finite element methods, is often quite large in practice. This situation contrasts with the so-called optimal approach, for which a low-order model is being searched for in a certain class, with a distance to be minimized between the infinite-dimensional ideal system and the low-order model. In this approach, two steps are of main interest, namely the choice of structure of the finite-dimensional model and the choice of the distance between these models.

The first step can be viewed as an off-line pre-processing of the physical model itself: it takes advantage of the flexibility of state-space representations for infinite-dimensional linear systems (Zwart, 2004). Transfer functions between inputs and outputs are first computed and then carefully analyzed using tools of complex variable theory (Duffy, 1994): for irrational transfer functions, the choice of appropriate cuts and poles, which are highly not unique, helps establish a state-space representation which reveals the very structure of the exact dynamical system to be simulated.

The second step consists in defining optimal low-cost representations of the exact one: choosing useful frequency points together with a measurement scale leads to user-oriented optimization procedures, which are carefully designed and driven by the underlying application. In the very end, a finite-dimensional discrete-time linear system is found to fit best for the on-line real-time simulation of the original system.

The paper is organized as follows: in § 2, a description of the systems under consideration is given; firstly their representation with poles and cuts is presented in § 2.1, secondly the structure of their finite-dimensional approximations is recalled in § 2.2. Based on these structures, specialized optimization procedures are derived in § 3: care is taken of the definition of the functional spaces and measures in § 3.1, whereas regularization procedures and equality constraints are presented in § 3.2. Three applications are then investigated in § 4: the first one is a somewhat academic example of fractional integral (§ 4.1), while the second one is a more involved example stemming from acoustics of ducts with viscothermal losses (§ 4.2). Finally in § 4.3, we show how to apply the whole methodology to a compound system decomposed into pure delays and elementary transfer functions that can be represented with poles and cuts; this last example gives rise to real-time simulations.

2. SYSTEMS UNDER CONSIDERATION

2.1 Representations with poles and cuts

2.1.1. General framework We consider linear systems with transfer functions which can be decomposed as follows, in some right-half complex plane $\mathbb{C}_a^+ = \left\{ s \in \mathbb{C} \,|\, \Re e(s) > a \right\}$,

$$H(s) = \sum_{k \in \mathcal{K}} \sum_{l=1}^{L_k} \frac{r_{k,l}}{(s - s_k)^l} + \int_{\mathcal{C}} \frac{M(\mathrm{d}\gamma)}{s - \gamma}, \quad (1)$$

where the set of poles $\mathcal{K}$ is finite. This translates in the time domain into the following decomposition of the impulse response, for $t > 0$,

$$h(t) = \sum_{k \in \mathcal{K}} \sum_{l=1}^{L_k} \frac{r_{k,l}}{l!} \, t^{l-1} \, e^{s_k \, t} + \int_{\mathcal{C}} e^{\gamma \, t} \, M(\mathrm{d}\gamma), \quad (2)$$

For systems which map real inputs to real outputs, transfer functions satisfy the hermitian symmetry $H(s) = \overline{H(\overline{s})}$, $s \in \mathbb{C}_a^+$. In this case, the same symmetry for the set of poles and the set $\mathcal{C}$ can be chosen for any analytic continuation of $(H(s) + \overline{H(\overline{s})})/2$; thus decompositions (1-2) can reduce to:

$$H(s) = \frac{1}{2} \sum_{k \in \mathcal{K}_+} \sum_{l=1}^{L_k} \left[\frac{r_{k,l,+}}{(s - s_k)^l} + \frac{\overline{r_{k,l,+}}}{(s - \overline{s_k})^l} \right]$$
$$+ \frac{1}{2} \int_{\mathcal{C}_+} \left[\frac{M_+(\mathrm{d}\gamma)}{s - \gamma} + \frac{\overline{M_+(\mathrm{d}\gamma)}}{s - \overline{\gamma}} \right], \quad (3)$$

$$h(t) = \Re e \left(\sum_{k \in \mathcal{K}_+} \sum_{l=1}^{L_k} \frac{r_{k,l,+}}{l!} \, t^{l-1} \, e^{s_k \, t} \right.$$
$$\left. + \int_{\mathcal{C}_+} e^{\gamma \, t} \, M_+(\mathrm{d}\gamma) \right), \quad (4)$$

for $t > 0$, where $\mathcal{K}_+ = \mathcal{K} \cap \mathcal{I}_+$ and $\mathcal{C}_+ = \mathcal{C} \cap \mathcal{I}_+$ with $\mathcal{I}_+ = \left\{ s \in \mathbb{C} \,|\, \Im m(s) \geq 0 \right\}$, and where $r_{k,l,+} = n_+(s_k) \, r_{k,l}$ and $M_+(\mathrm{d}\gamma) = n_+(\gamma) M(\mathrm{d}\gamma)$ with

$$n_+(s) = \begin{cases} 1 \text{ if } s \in \mathbb{R} \\ 2 \text{ otherwise} \end{cases} \quad (5)$$

This latter formulation could appear quite heavy at first glance, but presents many advantages: it ensures the hermitian symmetry; it also yields concise realizations in the time domain without redundancy; finally, it will prove most useful for optimization procedures.

The time-domain simulation of the *finite-dimensional part* of size $\sum_{k=1}^{K} L_k$ is really standard and will not be detailed in the sequel. The time-domain simulation of the *infinite-dimensional part* of these systems can quite easily be done through the following continuous family of *first-order differential systems*, parametrized by $\gamma \in \mathcal{C}_+$:

$$\partial_t \phi(\gamma, t) = \gamma \, \phi(\gamma, t) + u(t), \quad \phi(\gamma, 0) = 0, \quad (6)$$

$$y(t) = \Re e \left(\int_{\mathcal{C}_+} \phi(\gamma, t) \, M_+(\mathrm{d}\gamma) \right), \quad (7)$$

which is nothing but an *input u / state φ / output y* representation in the sense of systems theory.

In all the integral equations above, $\mathcal{C}$ is a contour in some left-half complex plane and M is a *measure* on this contour. Once a parametrization has been chosen for the contour, the measure can be decomposed into different parts, such as a purely discrete part (Dirac measures at some points in some left-half *complex* plane) and an absolutely continuous part $\mu(\gamma)$ with respect to the Lebesgue measure $d\gamma$. A straightforward interpretation can therefore be proposed: $\mu(\gamma)$ plays the role of the residue at the pole $s = \gamma$.

But of course, these representations make sense only if a *well-posedness condition* is fulfilled:

$$\int_{\mathcal{C}_+} \left| \frac{M_+(d\gamma)}{a+1-\gamma} \right| < \infty. \quad (8)$$

We refer to (Staffans, 1994, §5 and §6) for the general theory and (Matignon and Zwart, 2004) for the implications of the well-posedness condition.

When M has a density μ, and the curve $\mathcal{C}$ admits a $\mathcal{C}^1$-regular parametrization $\xi \mapsto \gamma(\xi)$ which is non-degenerate ($\gamma'(\xi) \neq 0$), an analytical computation of μ can be performed from H with

$$\mu(\gamma) = \lim_{\varepsilon \to 0^+} \frac{H(\gamma + i\gamma'\varepsilon) - H(\gamma - i\gamma'\varepsilon)}{2i\pi}. \quad (9)$$

Note that $\mu_+(\gamma) = n_+(\gamma)\,\mu(\gamma)$, $\gamma \in \mathcal{C}_+$ (cf. (5)).

2.1.2. Extension of the framework When the well-posedness condition (8) is not met, the representation (1) fails. Nevertheless, an extension can be proposed in some larger mathematical framework, that is, when $\breve{H}(s) = \big(H(s) - H(0)\big)/s$ admits a representation with $\breve{M}$ satisfying (8). This yields

$$H(s) = s \int_{\mathcal{C}} \frac{\breve{M}(d\gamma)}{s-\gamma} + H(0), \quad (10)$$

which gives rise to the following representation in the time domain, for $t > 0$ and $\gamma \in \mathcal{C}$:

$$\partial_t \phi(\gamma,t) = \gamma\,\phi(\gamma,t) + u(t), \quad \phi(\gamma,0) = 0, \quad (11)$$

$$z(t) = \int_{\mathcal{C}} \partial_t \phi(\gamma,t)\,\breve{M}(d\gamma) + H(0)\,u(t). \quad (12)$$

In the sequel, the notations $\mathcal{K}_+, \mathcal{C}_+, M_+$ and μ_+ are replaced by $\mathcal{K}, \mathcal{C}, M$ and μ respectively, for sake of conciseness.

2.2 Finite dimensional approximations in continuous and discrete time domain

2.2.1. Continuous time A first method consists in approximating $\phi(\gamma,t)$, $\gamma \in \mathcal{C}$ by

$$\widetilde{\phi}(\gamma,t) = \sum_{p=1}^{P} \phi_p(t)\,\Lambda_p(\gamma), \quad (13)$$

where $\phi_p(t) = \phi(\gamma_p,t)$, $(\gamma_p)_{0 \leq p \leq P+1}$ are sorted with respect to the oriented cut $\mathcal{C}$, and $\{\Lambda_p\}_{1 \leq p \leq P}$ defines *continuous piecewise linear interpolating functions* which are non zero on the piece $]\gamma_{p-1}, \gamma_{p+1}[_{\mathcal{C}}$ of the cut $\mathcal{C}$ and such that $\Lambda_p(\gamma_p) = 1$. Convergence results can be proven, see e.g. (Heleschewitz, 2000) for the purely diffusive case $\gamma = -\xi \in \mathbb{R}^-$.

The realizations (6-7) and (12) yield the first-order linear systems of dimension P ($\phi_p(0) = 0$),

$$\partial_t \phi_p(t) = \gamma_p\,\phi_p(t) + u(t), \; 1 \leq p \leq P, \quad (14)$$

$$\widetilde{y}(t) = \Re e \sum_{p=1}^{P} \mu_p\,\phi_p(t) \quad (15)$$

$$\text{with } \mu_p = \int_{[\gamma_{p-1},\gamma_{p+1}]_{\mathcal{C}}} \mu(\gamma)\Lambda_p(\gamma)\,d\gamma. \quad (16)$$

$$\text{or } \widetilde{z}(t) = \Re e \sum_{p=1}^{P} (\gamma_p \breve{\mu}_p)\phi_p(t) + \breve{\lambda}u(t), \quad (17)$$

$$\text{with } \breve{\lambda} = H(0) + \Re e \sum_{p=1}^{P} \breve{\mu}_p \quad (18)$$

where $\breve{\mu}_p$ is defined from $\breve{\mu}(\gamma)$ as in (16). Contribution of poles can be performed in the same way with standard finite-order systems, see e.g. (Dauphin *et al.*, 2000). Thus, the *general structure* of the approximated transfer function is

$$\widetilde{H}_\mu(s) = \frac{1}{2}\sum_{p=1}^{P} \left[\frac{\mu_p}{s-\gamma_p} + \frac{\overline{\mu_p}}{s-\overline{\gamma_p}} \right] + \breve{\lambda} \quad (19)$$

with the convention $\mu_p \in \mathbb{R}$ whenever $\gamma_p \in \mathbb{R}$ and where $\breve{\lambda} = 0$ in the non-extended case.

2.2.2. Discrete time We model $u(t)$ as the output of a causal interpolation filter of order Q fed by $\sum_{n \in \mathbb{N}} u_n \delta(t - nT_s)$. Classical examples are: a *sample and hold filter (SH)*, namely $u(t) \approx u_n$ for $t_n \leq t < t_{n+1}$, or a *linear interpolation (LI)*, namely $u(t) \approx u_n + \frac{t-t_n}{T_s}(u_{n+1} - u_n)$. Then, analytical solutions of (14-19) exist and yield discrete-time models of the form:

$$\phi_p(t_n) = \alpha_p\,\phi_p(t_{n-1}) + \sum_{q=0}^{Q} \beta_{p,q} u(t_{n-q}) \quad (20)$$

$$\widetilde{y}(t_n) = \Re e \sum_{p=1}^{P} \nu_p \phi_p(t_n), \quad (21)$$

$$\widetilde{z}(t_n) = \Re e \left(\sum_{p=1}^{P} \alpha_p \breve{\nu}_p \phi_p(t_n) + \breve{\lambda}u(t_n) \right) \quad (22)$$

with the (z-transformed) transfer function $\widetilde{H}_{\lambda,\alpha}(z) =$

$$\frac{1}{2}\sum_{p=1}^{P} \left[\frac{\sum_{q=0}^{Q} \lambda_{p,q} z^{-q}}{1 - \alpha_p z^{-1}} + \frac{\sum_{q=0}^{Q} \overline{\lambda_{p,q}} z^{-q}}{1 - \overline{\alpha_p} z^{-1}} \right] + \breve{\lambda} \quad (23)$$

where $\alpha_p = \mathrm{e}^{\gamma_p T_s}$, Q is the order of the filter, and T_s is the sampling period. Coefficients $\beta_{p,q}$ and ν_p are given in tab.1 for (SH) and (LI). Note that

	$\beta_{p,0}$	$\beta_{p,1}$	ν_p
SH	0	1	$\frac{\alpha_p - 1}{\gamma_p}\mu_p$
LI	1	$-\frac{\alpha_p(1-\gamma_p T_s)-1}{\alpha_p-(1+\gamma_p T_s)}$	$\frac{\alpha_p-(1+T_s\gamma_p)}{T_s\gamma_p}\mu_p$

Table 1. Coefficients $\beta_{p,q}$.

coefficients $\beta_{p,q}$ only depend on the choice of the interpolation method, while ν_p depends moreover on the transfer function through the weights μ_p.

3. SPECIALIZED OPTIMIZATION PROCEDURES

More accurate approximations can be performed by optimizing the weights μ_p rather than deriving them from the interpolated state (13), see e.g. (Garcia and Bernussou, 1998; Dunau, 2000). This section is dedicated to define distances that are adapted to each application, taking the performances of main interest into consideration.

3.1 Functional spaces and measures

Thanks to Parseval equality, the norm of a causal distribution h in Sobolev spaces H^s, with $s \in \mathbb{R}$, reads:

$$\|h\|^2_{H^s(\mathbb{R}_t)} = \int_{\mathbb{R}_f} (1 + 4\pi^2 f^2)^s |H(2\mathrm{i}\pi f)|^2 \,\mathrm{d}f$$

where H is the Laplace transform of h. Defining $d_s(h,\widetilde{h}) = \|h - \widetilde{h}\|_{H^s(\mathbb{R}_t)}$ gives a family of distances between ideal (h) and approximated ($\widetilde{h}$) systems, for which spectral weightenings $w_s(f) = (1 + 4\pi^2 f^2)^s$ act in very different ways. The case $s = 0$ corresponds to the classical L^2-norm, for which the weightening is uniform on the whole frequency range. The H^1-norm, which requires $h - \widetilde{h}$ to be a $\mathcal{C}^0$-function in the time domain, is more sensitive to high frequencies than low ones. This is the opposite for the H^{-1}-norm, which allows $h - \widetilde{h}$ to be a distribution. More generally, s can be seen as a tuning parameter of the low-and-high frequency balance.

Weightenings can also be viewed as the result of scalings: for instance, considering a logarithmic scale for frequencies, such as in Bode diagrams, results in choosing the measure $\mathrm{d}lnf = \mathrm{d}f/f$, which amounts to use $w(f) = 1/f$.

In practice, such considerations can be used to build *weightenings based on each application*. For instance, $w(f)$ can be adapted and modified according to the following requirements:

- a bounded frequency range $f \in [f^-, f^+]$: $w(f)\mathbf{1}_{[f^-,f^+]}(f)$;

- a frequency log-scale: $w(f)/f$;
- a relative error measurement: $w(f)/|H(2\mathrm{i}\pi f)|^2$
- a relative error on a bounded dynamics: $w(f)/\big(\mathrm{Sat}_{H,\Theta}(f)\big)^2$ where the saturation function $\mathrm{Sat}_{H,\Theta}$ with threshold Θ is defined by

$$\mathrm{Sat}_{H,\Theta}(f) = \begin{cases} |H(2\mathrm{i}\pi f)| & \text{if } |H(2\mathrm{i}\pi f)| \geq \Theta_H \\ \Theta_H & \text{otherwise} \end{cases}$$

with $\Theta_H = \Theta \sup_{\{f \,|\, w(f)\neq 0\}} |H(2\mathrm{i}\pi f)|$. Note that a $80\,\mathrm{dB}$-dynamics corresponds to $\Theta = 10^{-4}$;
- a conversion for the extension §2.1.2: the distance between h and $\widetilde{h}$ for $w(f)$ is the same as the distance between $\breve{h}$ and $\breve{\widetilde{h}}$ for the adapted weightening $4\pi^2 f^2\, w(f)$.

All these requirements can be cumulated in the appropriate order.

3.2 Regularized criterion with equality constraints

Such distances can lead to ill-conditionned problems. We use standard regularization techniques to cope with this (Walter and Pronzato, 1997), introducing the regularized criterion $\mathcal{C}_R(\mu)$:

$$\mathcal{C}_R(\mu) = \mathcal{C}(\mu) + \sum_{p=1}^{P} \epsilon_p |\mu_p|^2, \tag{24}$$

$$\mathcal{C}(\mu) = \int_{\mathbb{R}^+} \left| \widetilde{H_\mu}(2\mathrm{i}\pi f) - H(2\mathrm{i}\pi f) \right|^2 w(f)\,\mathrm{d}f. \tag{25}$$

The convention in (19) expresses a realness constraint. But rather than expressing it by means of a Lagrange multiplier, it is more straightforward to decompose the set of poles into the real ones ($1 \leq p \leq P_1$) and others ($1 \leq p - P_1 \leq P_2$ with $P = P_1 + P_2$), and to rewrite and optimize the criterion for the real parameters $\boldsymbol{\mu} = \left(\mu_1, ..., \mu_{P_1}, \Re\mathrm{e}(\mu_{P_1+1}), ..., \Re\mathrm{e}(\mu_P), \Im\mathrm{m}(\mu_{P_1+1}), ..., \Im\mathrm{m}(\mu_P)\right)^t \in \mathbb{R}^{P+P_2}$, as detailed in §3.3.

Nevertheless, in some applications, it is required for some derivatives $\widetilde{H_\mu}^{(d_j)}$ of an approximation $\widetilde{H_\mu}$ to be exact at prescribed frequency points η_j, $1 \leq j \leq J \leq \frac{1}{2}P_1 + P_2$. Such properties are achieved thanks to a Lagrangian criterion $\mathcal{C}_{R,L}$ by adding

$$\Re\mathrm{e}\left(\boldsymbol{\ell}^* \begin{bmatrix} H^{(d_1)}(2\mathrm{i}\pi\eta_1) - \widetilde{H_\mu}^{(d_1)}(2\mathrm{i}\pi\eta_1) \\ \vdots \\ H^{(d_J)}(2\mathrm{i}\pi\eta_J) - \widetilde{H_\mu}^{(d_J)}(2\mathrm{i}\pi\eta_J) \end{bmatrix} \right), \tag{26}$$

to (24), and optimizing with respect to both the $(P + P_2) \times 1$ vector $\boldsymbol{\mu}$, and $J \times 1$ vector $\boldsymbol{\ell} = \left[\ell_1, ..., \ell_J\right]^t \in \mathbb{C}^J$. We denote $\boldsymbol{\ell}^* \triangleq \overline{\boldsymbol{\ell}}^t$ as the transpose conjugate.

3.3 Numerical optimization

Numerically, the criterion (25) is computed for frequencies increasing from $f_1 = f_-$ to $f_{N+1} = f_+$, using the approximation

$$\mathcal{C}(\mu) \approx \sum_{n=1}^{N} w_n \left| \widetilde{H_\mu}(s_n) - H(s_n) \right|^2,$$

with $w_n = \int_{f_n}^{f_{n+1}} w(f)\,\mathrm{d}f$ and $s_n = 2\mathrm{i}\pi f_n$ for $1 \leq n \leq N$. Thus, with matrix notations, the criterion rewrites

$$\mathcal{C}_{R,L}(\boldsymbol{\mu}) = \left(\boldsymbol{M\mu} - \boldsymbol{h}\right)^* \boldsymbol{W} \left(\boldsymbol{M\mu} - \boldsymbol{h}\right) + \boldsymbol{\mu}^t \boldsymbol{E\mu}$$
$$+ \Re\!\left(\boldsymbol{\ell}^* \left[\boldsymbol{k} - \boldsymbol{N\mu}\right]\right), \qquad (27)$$

still with $\boldsymbol{M}^* \triangleq \overline{\boldsymbol{M}}^t$ and where

- $\boldsymbol{M}$ is an $N \times (P + P_2)$ matrix, with $M_{n,p} = \frac{1}{2}\left[\frac{1}{s_n - \gamma_p} + \frac{1}{s_n - \overline{\gamma_p}}\right]$ for $1 \leq p \leq P$, and $M_{n,p} = \frac{1}{2}\left[\frac{\mathrm{i}}{s_n - \gamma_{p-P_2}} - \frac{\mathrm{i}}{s_n - \overline{\gamma_{p-P_2}}}\right]$ for $1 \leq p - P \leq P_2$,
- $\boldsymbol{N}$ is a $J \times (P + P_2)$ matrix, with $N_{j,p} = \frac{(-1)^{d_j}}{2\,d_j!}\left[\frac{1}{(2\mathrm{i}\pi\eta_j - \gamma_p)^{d_j+1}} + \frac{1}{(2\mathrm{i}\pi\eta_j - \overline{\gamma_p})^{d_j+1}}\right]$ if $1 \leq p \leq P$, and if $P + 1 \leq p \leq P + P_2$, by $N_{j,p} = \frac{(-1)^{d_j}}{2\,d_j!}\left[\frac{\mathrm{i}}{(2\mathrm{i}\pi\eta_j - \gamma_{p-P_2})^{d_j+1}} - \frac{\mathrm{i}}{(2\mathrm{i}\pi\eta_j - \overline{\gamma_{p-P_2}})^{d_j+1}}\right]$,
- $\boldsymbol{E}$ is a $(P+P_2) \times (P+P_2)$ diagonal matrix, with $E_{p,p} = \epsilon_p$ for $1 \leq p \leq P$ and, $E_{p,p} = \epsilon_{p-P_2}$ for $P+1 \leq p \leq P+P_2$,
- $\boldsymbol{W}$ is the $N \times N$ diagonal matrix $\mathbf{diag}(w_n)$,
- $\boldsymbol{h}$ is the $N \times 1$ vector $h_n = H(s_n)$,
- $\boldsymbol{k}$ is the $J \times 1$ vector $k_j = H^{(d_j)}(2\mathrm{i}\pi\eta_j)$.

Solving this least squares problem with the constraint that $\boldsymbol{\mu}$ is real valued yields

$$\boldsymbol{\mu} = \mathcal{M}^{-1}\left[\mathcal{H} + \underline{\boldsymbol{N}}^t \mathcal{N}^{-1}\left(\underline{\boldsymbol{k}} - \underline{\boldsymbol{N}}\mathcal{M}^{-1}\mathcal{H}\right)\right], \quad (28)$$

where $\mathcal{M} = \Re\!\left(\boldsymbol{M}^*\boldsymbol{W}\boldsymbol{M} + \boldsymbol{E}\right)$, $\mathcal{H} = \Re\!\left(\boldsymbol{M}^*\boldsymbol{W}\boldsymbol{h}\right)$ and $\mathcal{N} = \underline{\boldsymbol{N}}\mathcal{M}^{-1}\underline{\boldsymbol{N}}^t$ with $\underline{\boldsymbol{N}}^t = [\Re(\boldsymbol{N}^t), \Im(\boldsymbol{N}^t)]$ and $\underline{\boldsymbol{k}}^t = [\Re(\boldsymbol{k}^t), \Im(\boldsymbol{k}^t)]$. Note that (28) reduces to $\boldsymbol{\mu} = \mathcal{M}^{-1}\mathcal{H}$ without constraints ($J = 0$) and that $\mathcal{N}$ is invertible for non-redundant constraints.

4. APPLICATION TO LOW-COST SIMULATION OF COMPLEX SYSTEMS

4.1 Example 1: an integral representation on $\mathbb{R}^-$

The causal integral operators of fractional order have irrational transfer functions $H(s) = s^{-\beta}$, $0 < \Re(\beta) < 1$, with impulse response $h(t) = t^{\beta-1}/\Gamma(\beta)$. Choosing $\mathcal{C} = \mathcal{C}_+ = \mathbb{R}^-$ and $\gamma = -\xi$ yields $\mu(-\xi) = \mu_+(-\xi) = \frac{\sin(\beta\pi)}{\pi}\frac{1}{\xi^\beta}$, which fulfills (8), see (Matignon, 1998) for details.

The interpolation method (13-16) is applied with a logarithmic grid from $\xi_{min} = 5.10^{-4}$ to $\xi_{max} =$

5.10^3, first for $P = 10$ ($\circ$), second for $P = 16$ ($\times$, see fig. 1ⓐ). Optimization is applied with $w_{BLR}(f) = \mathbf{1}_{[f^-, f^+]}(f)/(f\,|H(2\mathrm{i}\pi f)|^2)$, which corresponds to a bounded frequency range with a logarithmic scale, combined with a relative error measurement. Results with $P = 10$ only are much better than those of interpolation with $P = 16$ (see fig. 1ⓑ). Other examples with the same cut, such
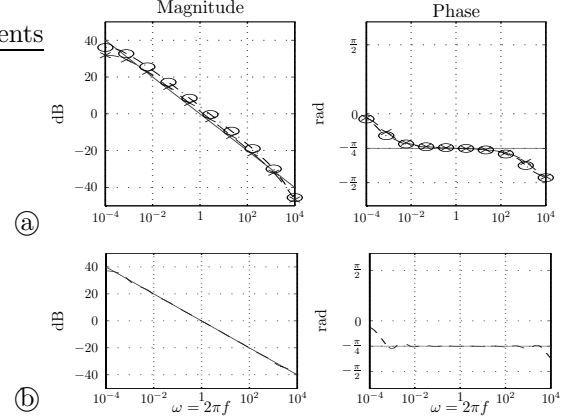

Fig. 1. ⓐ: interpolation. ⓑ: optimization.

as $\tanh(\sqrt{s})/\sqrt{s}$, s^α, $e^{-\sqrt{s}}/\sqrt{s}$ or $e^{-\sqrt{s}}$ detailed in (Hélie and Matignon, 2005b), prove optimization to be more efficient than interpolation.

4.2 Example 2: an integral representation on $\mathcal{C} \subset \mathbb{C}^-$

Some more intricate transfer functions can be met. This is the case for an acoustic bell, the transmission of which is accurately modelled (up to a global delay) by the transfer function H:

$$H(s) = \frac{2R(s)\,e^{s-R(s)}}{s + R(s)} \text{ with } R(s) = \sqrt{s^2 + \varepsilon\,s^{\frac{3}{2}} + 1},$$

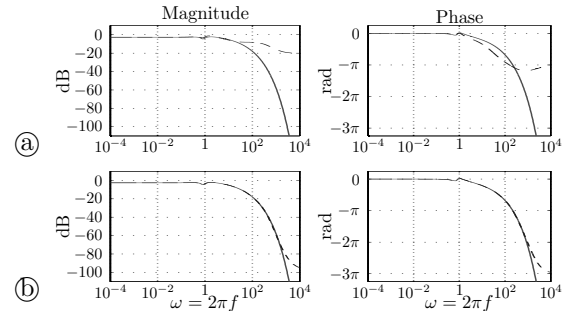where $\varepsilon > 0$ accounts for visco-thermal losses. This function is derived from a PDE with frac-

Fig. 2. ⓐ: interpolation. ⓑ: optimization.

tional derivatives (see (Hélie, 2003) for the model and (Haddar et al., 2003) for its theoretical study). It has 3 branching points $(0, s_1, \overline{s_1}$ with $\Re e(s_1) < 0)$; two different cuts are investigated (Hélie and Matignon, 2005a): $\mathcal{C} = \mathbb{R}^- \cup \left(s_1 + \mathbb{R}^-\right) \cup \left(\overline{s_1} + \mathbb{R}^-\right)$ and $\mathcal{C} = \mathbb{R}^- \cup [s_1, \overline{s_1}]$. Fig. 2 gives results for $(P_1, P_2) = (4, 8)$. The optimization yields accurate approximations on more than 7 decades and a dynamics of 80dB, with $w_{BLR}(f)$.

4.3 Example 3: a compound system with delays

A trumpet-like intrument has been built by chaining a cup, straight and flared pipes and a radiation impedance (Hélie *et al.*, 2003). Algebraic calculations allow to derive a structure composed of pure delays and quadripoles (Mignot, 2005) (see fig. 3). Quadripole $\mathcal{Q}_1$ involves 7 transfer functions with
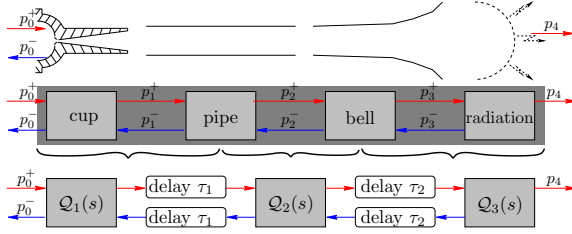

Fig. 3. Trumpet-like instrument

$\mathcal{C} = \mathbb{R}^-$ optimized on $[f_-, f_+] = [20\text{Hz}, 20\text{kHz}]$ with $w_{BLR}(f)$; one is extended (§ 2.1.2) and $P_1 = 7$; six are not and $P_1 = 5$. $\mathcal{Q}_2$ involves 11 transfer functions; three with $\mathcal{C} = \mathbb{R}^-$ and $P_1 = 5$; eight with $\mathcal{C} \subset \mathbb{C}^-$ and $(P_1, P_2) = (6, 8)$. $\mathcal{Q}_3$ involves 3 transfer functions with $\mathcal{C} \subset \mathbb{C}^-$ and $(P_1, P_2) = (0, 7)$.

A simulation in real-time has been performed in the Pure-Data environment, using circular buffers for delays and systems (20-22) with (LI)-filters. The impulse response of the transmission $(p_0^+ \mapsto p_4)$ is given in fig.4ⓐ for the sampling frequency $f_s = 44.1\text{kHz}$. A comparison between its Fourier transform (- -) and the exact transmission (-) is displayed on fig.4ⓑ. For Single-Input/Multiple-
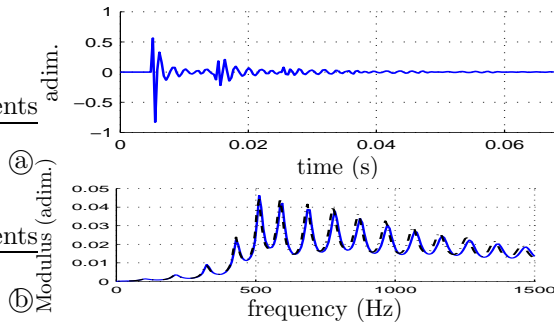

Fig. 4. Transmission. ⓐ: time. ⓑ: frequency.

Ouput systems approximated for the same poles, a cheap state-space representation shares a *common state* (20) from which each output is observed (21-22). This efficiently reduces the cost in $\mathcal{Q}_{1,2,3}$.

5. PERSPECTIVE

The reflexion function is badly approximated in the low frequency range because of its high sensitivity to both the value and the first derivative of transfer functions at $f = 0$. So far, adding a high-pass filter is required. Using equality constraints at $f = 0$ should properly overcome this problem.

REFERENCES

Dauphin, G., D. Heleschewitz and D. Matignon (2000). Extended diffusive representations and application to non-standard oscillators. In: *Mathematical Theory of Networks and Systems.* Perpignan, France. 10 p.

Duffy, D. G. (1994). *Transform methods for solving partial differential equations.* CRC Press.

Dunau, M. (2000). Représentations diffusives de seconde espèce. DEA Auto. Univ. Toulouse.

Garcia, G. and J. Bernussou (1998). Identification of the dynamics of a lead acid battery by a diffusive model. *ESAIM: Proc.* **5**, 87–98.

Haddar, H., Th. Hélie and D. Matignon (2003). A Webster-Lokshin model for waves with viscothermal losses and impedance boundary conditions: strong solutions. In: *Int. conf. on math. and numerical aspects of wave propagation phenomena.* INRIA. Finland. pp. 66–71.

Heleschewitz, D. (2000). Analyse et simulation de systèmes différentiels fractionnaires et pseudo-différentiels linéaires sous représentation diffusive. PhD thesis. ENST.

Hélie, Th. (2003). Mono-dimensional models of the acoustic propagation in axisymmetric waveguides. *J. Acoust. Soc. Amer..* **114**, 2633–2647.

Hélie, Th. and D. Matignon (2005a). Diffusive reprentations for the analysis and simulation of flared acoustic pipes with visco-thermal losses. *Mathematical Models and Methods in Applied Sciences (M3AS).* to appear.

Hélie, Th. and D. Matignon (2005b). Representations with poles and cuts for the time-domain simulation of fractional systems and irrational transfer functions *Signal Processing.* to appear.

Hélie, Th. and X. Rodet (2003). Radiation of a pulsating portion of a sphere: application to horn radiation. *Acta Acustica.* **89**, 565-577.

Matignon, D. (1998). Stability properties for generalized fractional differential systems. *ESAIM: Proc.* **5**, 145–158.

Matignon, D. and H. Zwart (2004). Diffusive systems as well-posed linear systems. In: *Mathematical Theory of Networks and Systems.* Leuven, Belgium.

Mignot, R. (2005). Simulation de propagation d'ondes dans les tubes évasés avec pertes visco-thermiques pour la synthèse sonore en temps réel . Master SDI. Univ. Paris VI.

Staffans, O. J. (1994). Well-posedness and stabilizability of a viscoelastic equation in energy space. *Trans. AMS.* **345**(2), 527–575.

Walter, E. and L. Pronzato, (1997). *Identification of parametric models from experimental data.* Springer-Verlag.

Zwart, H. (2004). Transfer functions for infinite-dimensional systems. *Systems & Control Letters* **52**(3-4), 247–255.